NEWS FROM THE STRONG INTERACTIONS PROGRAM OF NA61/SHINE* **

Angelika Tefelska

for the NA61/SHINE Collaboration

Warsaw University of Technology, Faculty of Physics, Poland

The NA61/SHINE experimental physics program focuses on searching for the critical point and studying the properties of the onset of deconfinement in the strongly interacting matter. A two-dimensional scan is performed by varying the beam momentum (from $13A$ to $150/158A$ GeV/c) and the system size (from $p+p$ to Pb+Pb) of the collided nuclei. This contribution presents the most recent results from the NA61/SHINE strong interactions program and includes future data-taking and analysis plans.

1. Introduction

The NA61/SHINE is a large acceptance, fixed target experiment, which uses eight Time Projection Chambers and a Time-of-Flight detector to identify the produced particles and measure their momenta. The collision centrality is determined based on measurements from the high-resolution forward calorimeter, the Projectile Spectator Detector (PSD).

The large variety of beams and targets allowed to perform two-dimensional scan by varying the beam momentum (from $13A$ to $150/158A$ GeV/c) and the system size (from $p+p$ to Pb+Pb) of the collided nuclei. The main goals of the strong interactions program are searching for the critical point of strongly interacting matter and studying the properties of the onset of deconfinement.

A. Tefelska

2. Study of the properties of the onset of deconfinement

The Statistical Model of the Early Stage [1] assumes a first-order phase transition from the hadronic matter to the Quark–Gluon Plasma (QGP) between top AGS ($\sqrt{s_{NN}} \approx 5$ GeV) and top SPS ($\sqrt{s_{NN}} \approx 17$ GeV) energies.

One of the predicted signatures of the deconfinement transition is horn, a non-monotonic change of K^+/π^+ ratio as a function of collision energy. The horn structure was observed by the NA49 experiment in central Pb+Pb collisions [2]. The NA61/SHINE extends the set of experimental data by $p+p$, Be+Be, and Ar+Sc collisions (Xe+La and Pb+Pb results are expected soon). The compilation of NA61/SHINE and world data is shown in Fig. 1. The plateau-like structures are visible in $p + p$ and Be+Be interactions at SPS energies. The K^+/π^+ ratio for Ar+Sc collisions is located between $p+p$ and Pb+Pb data but no horn-like structure is visible.
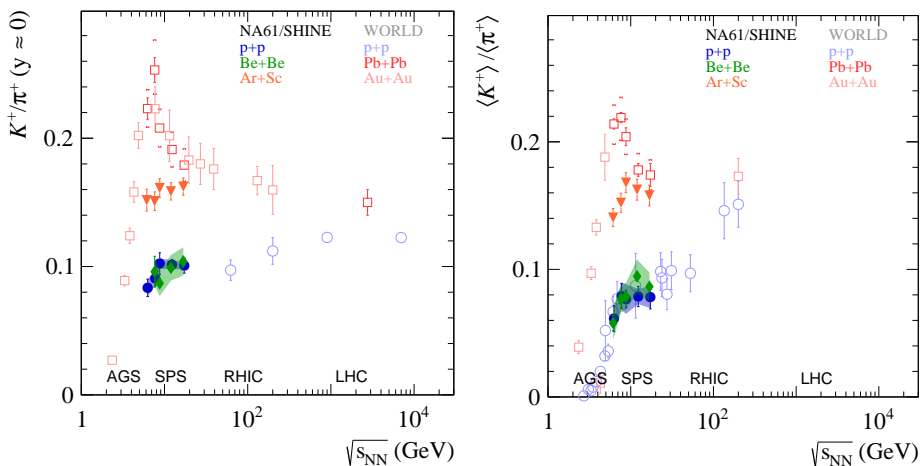

Fig. 1. The energy dependence of the K^+/π^+ particle yields ratio at mid-rapidity (left) and full acceptance (right) for the 20% most central Be+Be, central Pb+Pb, and Au+Au collisions, as well as inelastic $p + p$ interactions. The NA61/SHINE $p + p$ and Be+Be results are taken from Refs. [3, 4], whereas Ar+Sc points [5] are preliminary.

The K^+/π^+ ratio at mid-rapidity and inverse slope parameter T fitted to the transverse momentum spectra of K^+ mesons as a function of system size are shown in Fig. 2. All plots show similar, threshold-like behavior, which cannot be reproduced by any of the considered models. The observed rapid change of hadron production properties that starts when moving from Be+Be to Ar+Sc collisions at top SPS energies hints at the beginning of the creation of large clusters of strongly interacting matter called *the onset of fireball*.
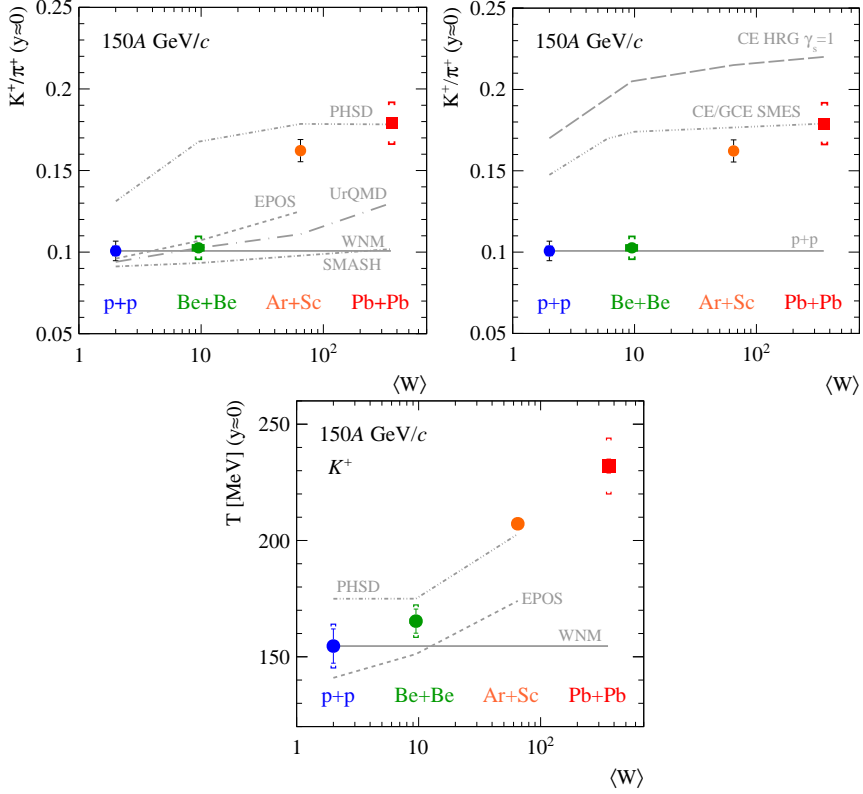
Fig. 2. Top: The system-size dependence of the K^+/π^+ ratio at mid-rapidity measured in NA61/SHINE $p+p$, Be+Be, Ar+Sc, and NA49 Pb+Pb collisions at $150A$ (Be+Be, Ar+Sc) or $158A$ ($p+p$, Pb+Pb) GeV/c compared with dynamical (top left) and statistical (top right) models. Bottom: The inverse slope parameter T, fitted to K^+ transverse momentum spectra at the similar collision energy [5]. The NA61/SHINE $p+p$ and Be+Be results are taken from Refs. [3, 4], whereas Ar+Sc points [5] are preliminary.

3. Search for the critical point

The critical point (CP) signal should be visible as a non-monotonic dependence of various fluctuation/correlation measures. Figure 3 shows the energy dependence of fluctuations for negatively charged hadrons (h^-) and net-electric charge ($h^+ - h^-$), measured in $p+p$, Be+Be, and Ar+Sc collisions. The comparison of fluctuations in systems of different sizes is possible using intensive quantities. For h^-, one considers ratios of cumulants $\kappa_2/\kappa_1[h^-]$ (scaled variance), $\kappa_3/\kappa_2[h^-]$ (scaled skewness), and $\kappa_4/\kappa_2[h^-]$ (scaled kurtosis) (reference value of 1 is defined by the Poisson distribution). In the case of net-electric charge, the first two ratios are slightly modified to keep the ref-

erence value (1 for the Skellam distribution): $\kappa_2[h^+ - h^-]/(\kappa_1[h^+] + \kappa_1[h^-])$, $\kappa_3/\kappa_1[h^+ - h^-]$. Figure 3 shows that in the case of h^-, only the scaled variance presents significant differences between heavier and lighter systems. In the case of net-electric charge, the scaled skewness and scaled kurtosis suggest a non-monotonic behavior, within sizeable systematic uncertainties (current subject of analysis).
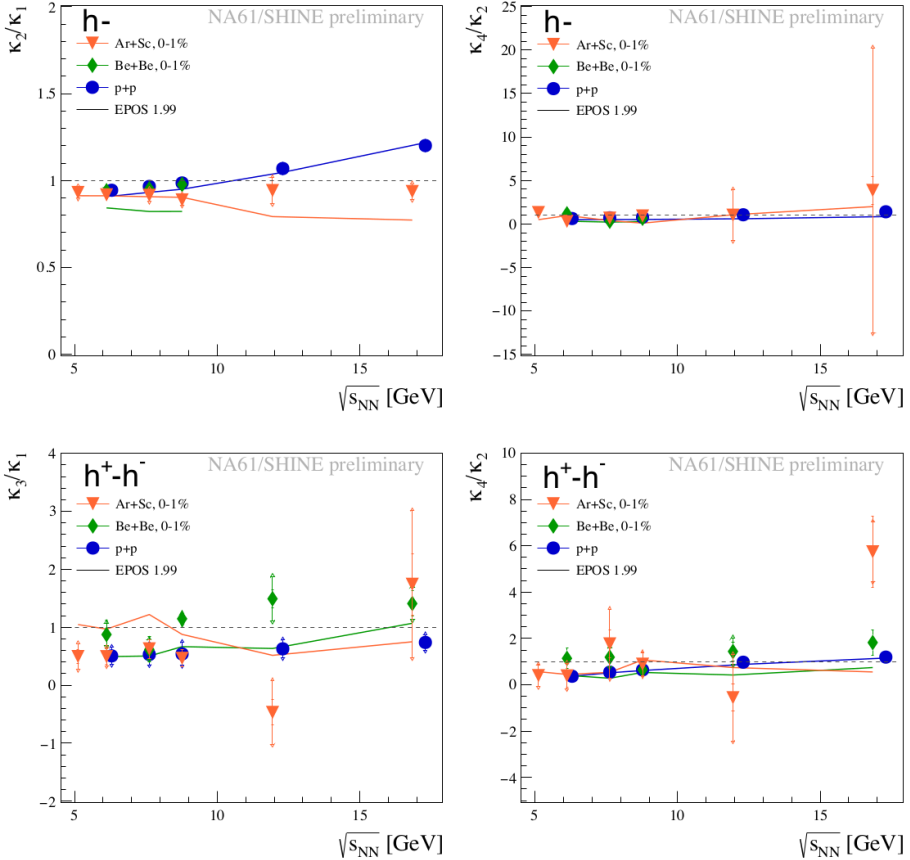

Fig. 3. Preliminary results on the energy dependence of fluctuations for negatively charged hadrons (top) and net-electric charge (bottom) in $p+p$, Be+Be, and Ar+Sc collisions.

Another possible tool for the search for CP is an intermittency analysis. Generally, the scaled factorial moments F_r are calculated based on the counted particles in cells in transverse momentum space [6]. If the system freezes out in the vicinity of the critical point, the scaled factorial moments should reveal a power-law dependence: $F_r(M) \sim M^{\phi_r}$, where M is the number of cells [7]. In this analysis, the statistically-independent points are

used and instead of the (p_x, p_y) cells, the cumulative variables are used to remove the dependence of the moments on the momentum distribution [8]. Preliminary results on $F_2(M)$ of mid-rapidity protons measured in the 0–20% most central Ar+Sc collisions at $150A$ GeV/c and 0–10% most central Pb+Pb collisions at $13A$ GeV/c are presented in Fig. 4 (top panels). The negatively charged hadron intermittency in 0–10% central Pb+Pb collisions at $30A$ GeV/c beam momentum up to the fourth scaled factorial moment is also shown in Fig. 4 (bottom panel). The measured $F_2(M)$ of protons for Ar+Sc at $150A$ GeV/c and Pb+Pb at $13A$ GeV/c, as well as $F_2(M)$, $F_3(M)$, and $F_4(M)$ of negatively charged hadrons in Pb+Pb at $30A$ GeV/c show no indication for power-law increase with a bin size which could indicate CP.
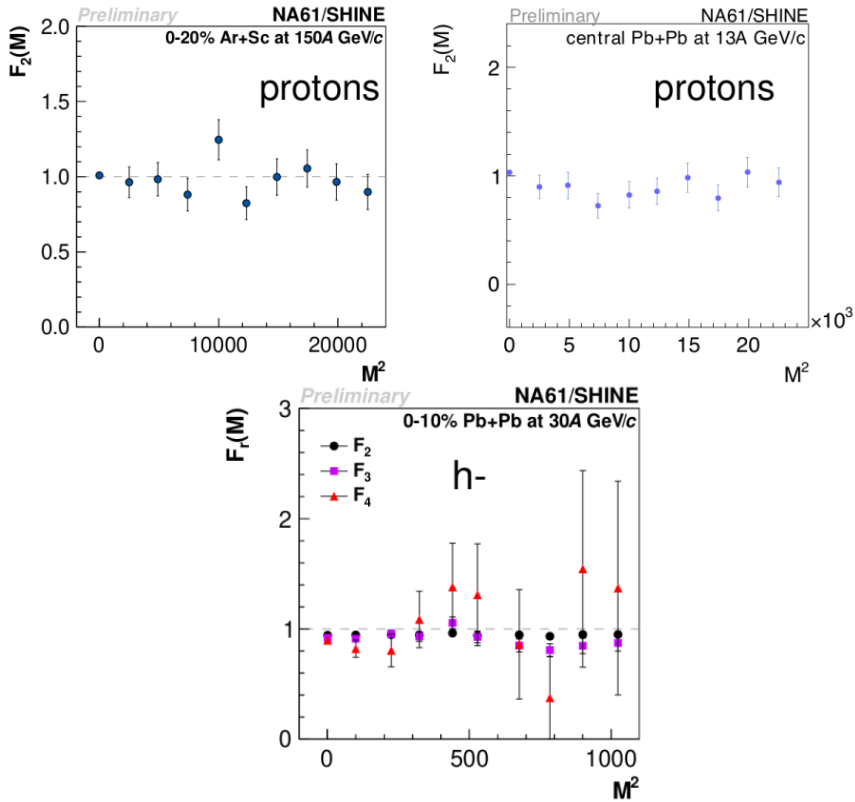

Fig. 4. Top: Preliminary results on intermittency analysis of mid-rapidity protons for the 0–20% most central Ar+Sc collisions at $150A$ GeV/c (top left) and 0–10% most central Pb+Pb collisions at $13A$ GeV/c (top right). Bottom: Preliminary results on intermittency analysis of mid-rapidity negatively charged hadrons for the 0–10% most central Pb+Pb collisions at $30A$ GeV/c.

The last topic connected with searching for CP are symmetric Lévy HBT correlations for the same-charge pion pairs in central Be+Be and Ar+Sc collisions at $150A$ GeV/c beam momentum. Usually, the correlation function assumes a Gaussian source but it can be generalized by the Lévy-shaped formula, $C(q) = 1 + \lambda\,e^{-(qR)^\alpha}$, where the parameter α describes the shape of the source (for $\alpha = 2$, the source is Gaussian, for $\alpha = 1$, the source is described by the Cauchy distribution). For the critical system, the α parameter should be equal to 0.5 according to the prediction of the 3D Ising model [9]. The α parameter as a function of transverse mass is shown in Fig. 5. The results do not indicate the critical point in Be+Be and Ar+Sc collisions. The values of α parameters are between Gaussian and Cauchy shapes and might be a sign of anomalous diffusion. The R Lévy scale parameter is also presented in Fig. 5 and describes the length of homogeneity. The visible transverse mass dependence can be a sign of transverse flow.
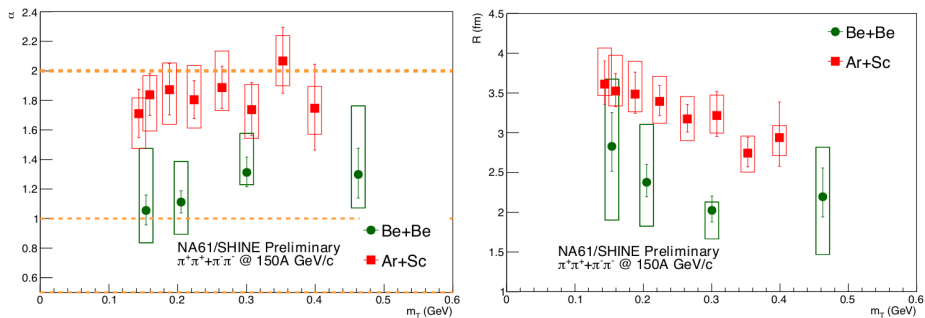

Fig. 5. Preliminary results on the symmetric Lévy HBT correlations for the same-charge pion pairs in central Be+Be and Ar+Sc collisions at $150A$ GeV/c beam momentum. The panels show the dependence of the α (left) and R (right) parameters on the transverse mass of the pair.

4. New data on hadron spectra in $p + p$ reactions

Finally, NA61/SHINE provides new and unique results on strangeness production in $p + p$ interactions. The spectra of strange mesons and multi-strange hyperons were measured with unprecedented precision at the SPS energy range. Figure 6 presents the rapidity distributions of $K^*(892)^0$ [10] and K_S^0 mesons (Ref. [11] and preliminary results) produced in inelastic $p+p$ interactions at the SPS energies.

The high-statistics data of $p + p$ collisions at 158 GeV/c allowed the more challenging measurement of $\Xi(1530)^0$ and $\bar{\bar{\Xi}}(1530)^0$ hyperon production [12], which are the only such results at the SPS energy. The first two-dimensional spectra of $\Xi(1530)^0$ and $\bar{\bar{\Xi}}(1530)^0$ [12] in y and p_T bins are presented in Fig. 7.
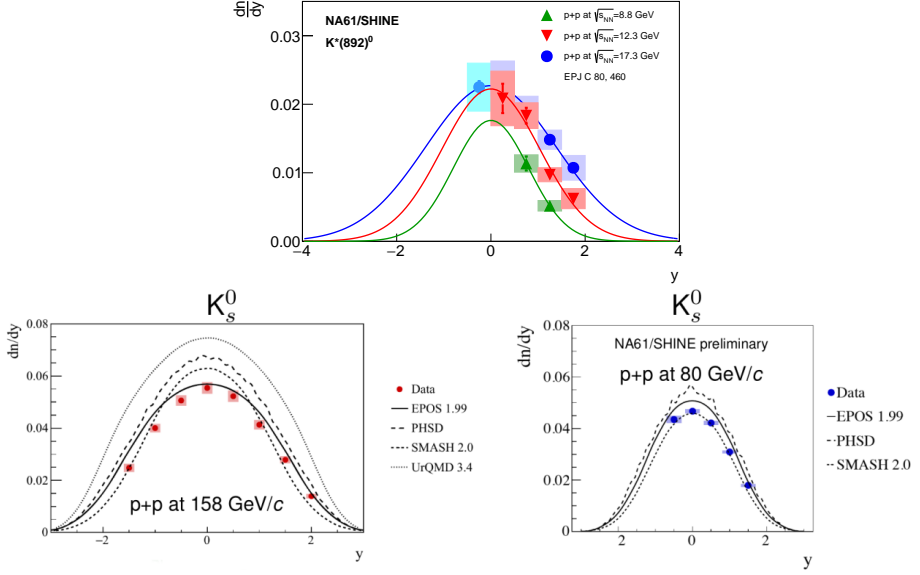
Fig. 6. Rapidity distributions of $K^*(892)^0$ (top) produced in inelastic $p + p$ interactions at 40–158 GeV/c [10] and K_S^0 produced in inelastic $p + p$ collisions at 158 GeV/c [11] (bottom left) and 80 GeV/c (bottom right). K_S^0 results at 80 GeV/c are preliminary.
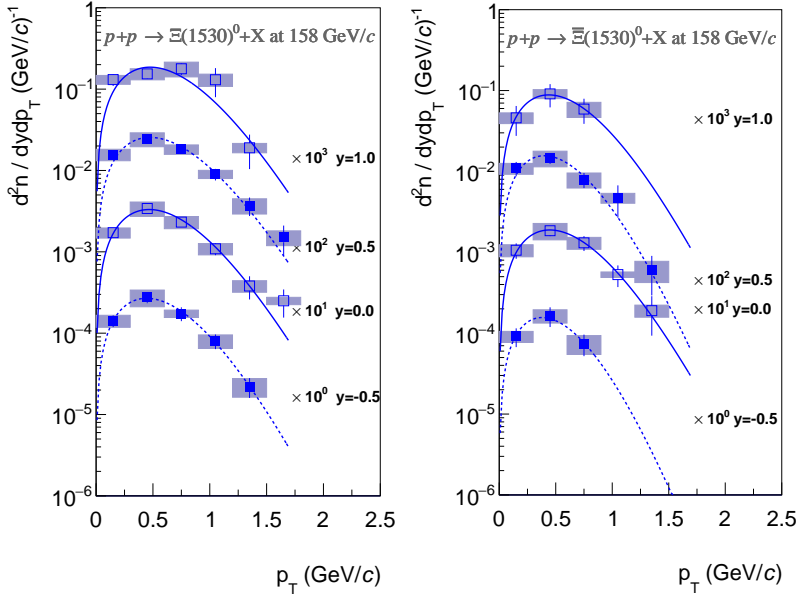

Fig. 7. Transverse momentum spectra in rapidity intervals of $\Xi(1530)^0$ and $\bar{\Xi}(1530)^0$ production in inelastic $p + p$ collisions at 158 GeV/c [12].

REFERENCES

[1] M. Gaździcki, M.I. Gorenstein, *Acta Phys. Pol. B* **30**, 2705 (1999).

[2] NA49 Collaboration (C. Alt *et al.*), *Phys. Rev. C* **77**, 024903 (2008).

[3] NA61/SHINE Collaboration (A. Aduszkiewicz *et al.*), *Phys. Rev. C* **102**, 011901 (2020).

[4] NA61/SHINE Collaboration (A. Acharya *et al.*), *Eur. Phys. J. C* **81**, 73 (2021).

[5] M.P. Lewicki, `arXiv:2212.06539 [nucl-ex]`.

[6] NA61/SHINE Collaboration (H. Adhikary *et al.*), CERN-SPSC-2022-034, 2022.

[7] N.G. Antoniou, F.K. Diakonos, A.S. Kapoyannis, K.S. Kousouris, *Phys. Rev. Lett.* **97**, 032002 (2006).

[8] A. Bialas, M. Gazdzicki, *Phys. Lett. B* **252**, 483 (1990).

[9] T. Csörgő, S. Hegyi, W.A. Zajc, *Eur. Phys. J. C* **36**, 67 (2004).

[10] NA61/SHINE Collaboration (A. Acharya *et al.*), *Eur. Phys. J. C* **82**, 322 (2022).

[11] NA61/SHINE Collaboration (A. Acharya *et al.*), *Eur. Phys. J. C* **82**, 96 (2022).

[12] NA61/SHINE Collaboration (A. Acharya *et al.*), *Eur. Phys. J. C* **81**, 911 (2021).